

Star/Galaxy Separation Revisited : Into the Zone of Avoidance

Avi Naim

Dept. of Physics, Carnegie-Mellon University, 5000 Forbes Ave., Pittsburgh, PA 15213

12 January 2019

ABSTRACT

The problem of automated separation of stars and galaxies on photographic plates is revisited with two goals in mind : First, to separate galaxies from everything else (as opposed to most previous work, in which galaxies were lumped together with all other non-stellar images). And second, to search optically for galaxies at low Galactic latitudes (an area that has been largely avoided in the past). This paper demonstrates how an artificial neural network can be trained to achieve both goals on Schmidt plates of the Digitised Sky Survey. Here I present the method while its application to large numbers of plates is deferred to a later paper. Analysis is also provided of the way in which the network operates and the results are used to counter claims that it is a complicated and incomprehensible tool.

1 INTRODUCTION

The separation of stars from galaxies on photographic plates or CCDs is required in large surveys like the APM survey (Maddox *et al.* 1990a) and the Sloan Digital Sky survey (Gunn 1995), for purposes such as the preparation of target lists of galaxies for observations (e.g., in order to obtain redshifts). The sheer number of detected objects on survey plates forces one to use automated procedures for this task and in every large survey some such method is chosen. It is generally relatively easy to separate single images of stars from everything else, and different methods have been successfully tried in order to achieve this goal. The DAOFIND package (e.g., as incorporated in IRAF) fits point spread functions to detect stars. Sebok (1979) uses surface brightness measurements from the image and matches them to templates of stars and various galaxy models. Jarvis and Tyson (1981) define shape parameters on the basis of image moments. Slezak *et al.* (1988) combine light profile with shape parameters, while the APM survey team (Maddox *et al.* 1990a) use automated parameters derived from the APM microdensitometer.

Regardless of which parameters are measured, the problem is usually formulated in terms of finding an optimal decision surface in the space spanned by the chosen parameters. This approach implies supervised learning by the classifier, i.e., learning from examples that were pre-classified, e.g., by eye. An alternative approach was recently proposed by Mähönen & Hakala (1995), who use an unsupervised learning method (self organising maps) to separate images on the basis of their appearance without classifying them by eye first. While promising, their approach was only demonstrated on synthetic images and is yet to be applied to real

images. In this paper supervised learning was preferred. The typical output of a classifier is the drawing of linear boundaries which distinguish between stars and non-stellar images, and it is usually assumed that the vast majority of all non-stellar objects in the field are galaxies.

There are at least three points that require further consideration when constructing yet another star/galaxy classifier :

- (i) Which parameters are adequate for describing galaxies and stars ?
- (ii) Is linear classification good enough ?
- (iii) Is it true that non-stellar objects are mostly galaxies ?

Although important, the first question is difficult to answer. Different parameters are measured by different researchers who do not all use the same plate material or even the same classification tools. Since the end result is a combination of all of these factors it is difficult to examine the effect of parameter choice separately. Because of this difficulty this paper makes no attempt to compare the parameters used here with those chosen by others. Rather, I augment parameters which were used successfully elsewhere (Odewahn *et al.* 1992) by several special-purpose parameters.

The second question requires careful comparison of linear and non-linear classifiers, using the same parameters and the same plate material. In many cases linear separation of stellar from non-stellar objects in the selected parameter space appears adequate (as judged by the distribution of galaxies and stars in plots of one parameter against another). However, in general a non-linear classifier is capable of at least as good a classification as a linear classifier, and thus the choice of a non-linear classifier seems natural. This paper follows Odewahn *et al.* in selecting artificial neural networks as the (non-linear) classifier.

As for the third question, it is shown below that galaxies do not dominate the population of non-stellar objects : the incidence of galaxies among non-stellar images is less than 50% even at high Galactic latitudes. This implies that treating “non-stars” as “galaxies” is in general wrong. Among the many non-stellar images on a typical plate one finds images of two or more overlapping stars which create elongated shapes; plate defects (e.g., scratches); meteorite trails; and combinations of the above with true galaxies. The fraction of galaxies drops significantly as one moves to low Galactic latitudes, making the problem worse still.

The aim of this paper is to extend previous work in two respects : first, by constructing a classifier that is capable of telling galaxies from all other objects. Discriminating between merged and extended objects is not an easy task and is largely ignored in this field. A notable exception is the work done by the APM team (Maddox *et al.* 1990a), who constructed two special parameters for telling merged objects apart from single objects. I attempt to carry this distinction further, by training the ANN to tell apart six different classes of object. The second respect in which previous work is extended is by making the classifier general enough to handle star/galaxy separation at low Galactic latitudes. The reason why one would wish to extend high latitude work into the *zone of avoidance* is the difficulty of using standard techniques to detect galaxies optically behind the disk of the Galaxy. The potential for new discoveries in that part of the sky has been realised several times in the past few decades, most recently in the radio band by Kraan-Korteweg *et al.* (1994). An optical identification of galaxy candidates could help save a lot of time in the search for partially obscured galaxies.

This paper serves to introduce the problem and the chosen method. The ultimate goal is the production of an automated catalogue of galaxy candidates behind the Galactic disk. The catalogue will be described in a later paper, which will also address issues of data quality, plate to plate changes and the overall reliability of the classifications. The data used for this first paper are described in § 2. § 3 describes the eyeball classification of the images. The parameters chosen to represent each image are discussed in § 4 and put to use in training the ANN, in § 5. The discussion follows in § 6.

2 THE DATA

The Digitised Sky Survey (DSS, Lasker *et al.* 1990) is a collection of digitised plates, taken with the UK Schmidt Telescope in Australia (southern sky, blue band) and with the Hale telescope at Mount Palomar (the POSS I survey of the northern sky, red band). The plates were digitised at a low resolution in the first generation of the DSS, and the information distributed on CD-ROM discs. A second generation of higher resolution scans is currently in production. For the investigation of automated star/galaxy separation in this paper I used the DSS mk I collection of 61 discs covering the southern skies. The resolution of the PDS scanner used in the digitisation was $1.7 \text{ arcsec pixel}^{-1}$, so a reasonable lower limit on the size (major axis length) of treated images was set at $15''$. This roughly corresponds to a semi-major axis of 4.5 pixels, and allows one to get some structural detail even from the smallest objects in the sample. The UK Schmidt plates are the same plates used for the APM survey, and the reader may obtain a full description of the quality and uniformity of the data in their papers (e.g., Maddox *et al.* 1990a; 1990b). In order to get an estimate of the magnitudes of the detected objects let us use a relation derived by the APM team (S. Maddox, private communication) :

$$(1) \quad \log(\text{Area}/(1'')^2) = 8.024 - 0.324 b_j$$

where b_j is the blue magnitude in the plate. This relation is derived for magnitudes between 13.5 and 19. It is not very tight for extended objects, and should therefore be used only as a rough guide to the magnitudes involved. At the limiting size of $15''$ a round object then has a rough magnitude of 17.8.

Considerations of the memory required by a reduction program forced a limit of about 1 deg^2 on any single patch of sky retrieved from the discs. In order to allow for images on the edges of any given patch the actual patches extracted were square, $70'$ on the side, having an overlap of $5'$ with patches on every side. The image itself then took up 12 Mb of memory, and various tables which were required for the reduction process increased the overall size of the program to roughly 40 Mb. Initially data were extracted for 25 patches making up field 646 of the UK Schmidt survey (centered on RA, DEC (1950): 13h, -15°). These patches are situated at a high Galactic latitude (the center of the field is at latitude 50°), so no problems such as overcrowding by stars or significant extinction were anticipated. Figure 1 shows a square section, 512 pixels on the side, of one of these patches. This corresponds roughly to a section 15 arcmin on the side. There are two adjacent scratches (bottom center) and at least three galaxies in this patch. There are several “stellar mergers” (images of two or more stars overlapping each other) as well. The patch is not very crowded and there are no mergers of more than three objects. In contrast, figure 2 shows another square section, 512 pixels on the side, of one of the patches at low galactic latitude (to be described below). This patch contains many more objects than the high latitude patch. There are numerous stellar mergers in it, and it is difficult to find a galaxy that does not merge into one or more stars.

Ten more patches were extracted from the DSS. Five were taken at Galactic latitude of around 15° (RA around 13 hours and DEC -47.5°) and five at Galactic latitude of about 5° (RA centered on 13 hours and DEC on -57.5°). The quality of the images was expected to be poorer, due to Galactic extinction at these latitudes and crowding by stars. This is seen clearly in figure 2. Upon careful inspection it was obvious that the smaller images contained a lot of spurious structure, and their shapes were affected badly. It was very difficult to assign certain eyeball classifications for images smaller than $25''$. For this reason, a lower limit of $25''$ was imposed on the size of all images to be eyeballed. Using the relation (1) this implies a limiting magnitude for round objects of roughly 16.5, more than a magnitude brighter than the limit of the high latitude objects.

3 EYEBALL CLASSIFICATION

At high Galactic latitudes all 6240 objects larger than $15''$ were classified by eye. Each object was assigned one of six possible classes:

Table 1. Distribution of Eyeball Classes in the Data Sets of field 646 (center at RA,DEC (1950): 13h, -15°; b = 50°.)

Class	Set 1	Set 2	Total
Star	1560	1551	3111
Galaxy	650	652	1302
Noise	102	94	196
Stellar Merger	613	615	1228
Star-Galaxy Merger	184	190	374
Galaxy Merger	11	18	29

Table 2. Distribution of Eyeball Classes in the Low Latitude Data Sets.

Class	Set 3	Set 4	Total
Star	52	60	112
Galaxy	10	12	22
Noise	6	5	11
Star Merger	383	384	767
Star-Galaxy Merger	61	54	115
Galaxy Merger	2	0	2

- (i) Star
- (ii) Galaxy
- (iii) Noise (e.g., scratches on the plate)
- (iv) Merger of two or more stellar images
- (v) Merger of one or more stellar image(s) and a galaxy image
- (vi) Merger of two or more galaxy images

A classification was forced even in the few cases where it was not entirely certain. An object would be assigned the class “stellar merger” even if it there was a significant difference in the apparent sizes of both stars. On the other hand, the star-galaxy merger class was assigned only to images in which the star was not much smaller than the galaxy. This was done because any galaxy image which is not severely contaminated by that of a star contains enough of the galaxy to allow its analysis and possibly even a detailed morphological classification. The distinction between a galaxy and a star-galaxy merger was therefore a little fuzzy, and could contribute some noise to the classification set.

The distribution of classifications of the 6240 objects at high Galactic latitude is described in table 1. These objects were randomly divided between two sets (sets 1 and 2 hereafter), each containing 3120 images. The breakdown of each of these sets into classes is also shown in table 1. As expected, stars are the most common class. There are quite a few galaxies, but even at such high Galactic latitudes the number of stellar mergers is quite *comparable to the number of galaxies*. If one were to distinguish only stars from everything else in these sets, galaxian objects would make up only around 54% of the “non-stellar objects” class.

At low Galactic latitudes all objects larger than 25” were classified by eye. The higher density of objects in these regions implied a very high number of objects, but the imposition of the higher size limit cut this number down to 1029. Again, these objects were divided to two sets of nearly equal sizes (hereafter sets 3 and 4). The distribution of classifications in these sets is shown in table 2, and figure 3 shows the frequencies of eyeball classes in the high-latitude patches and in the low-latitude patches. The excess of merged objects as one goes to lower latitudes is evident. The predominant class by far at low latitudes is the stellar-merger class, making galaxies a rather rare exception among non-stellar images.

4 DATA REDUCTION AND PARAMETER DESCRIPTIONS

The reduction program used on the APM galaxy images (Naim *et al.* 1995) was modified for the purpose of reducing these patches, although its principles remained the same: the sky level was obtained and subtracted and a list of all isolated groups of linked pixels was created. Each such group will be referred to as an “object”

hereafter, although many of them contain several merged objects. A set of 17 parameters was measured for each of the objects. Many of these parameters had been defined and used successfully for star/galaxy separation by Odewahn *et al.* (1992). These are listed below:

- log Area: The logarithm of the number of pixels in the object.
- Peak Intensity: Highest intensity of any pixel in the object.
- Average Intensity: Average intensity of all pixels in the object.
- Ellipticity and Position Angle: Object ellipticity and position angle of the major axis, calculated from the intensity-weighted second moments matrix of the image. Position angle not used to train the ANN.
- Semi-major Axis Length: Obtained from the distance (along the major axis) from the center of the object to its edge.
- Spike Trace: The ratio of the area implied by the extent of the object in the x and y directions of the picture to the area from pixel count. This ratio is sensitive to the existence of diffraction spikes, which extend along the x and y directions.
- The following moment:

$$(2) \quad I_1 = \frac{\sum_i I(r_i)/r_i}{\sum_i I(r_i)},$$

where $I(r_i)$ is the intensity at a given value of r_i , and r_i is the semi-major axis of the elliptical ring to which point i belongs. Both summations are over all pixels in the object.

- Light Gradients: In analogy with the sampled ellipses of the APM galaxy images, here only four ellipses were sampled and averaged to give a crude light profile consisting of four values. Five differences of intensities between pairs of ellipses were calculated as the gradients: The gradients between the pairs (1,2), (1,3), (1,4), (2,4) and (3,4) were used. This choice was made following Odewahn *et al.* (1992).

In addition to the above list several further parameters were designed to address the issue of classifying merged objects as separate from single stars and galaxies. These are the new parameters:

- Average Separability of Intensity Peaks: A list of local intensity maxima in the object was created, and a measure of how low the intensity dropped between any two such maxima was calculated. This measure was defined as I_{min}/I_{peaks} where I_{min} was the lowest intensity found along the line connecting the two peaks, and I_{peaks} was the average intensity of the two peaks. The parameter “average separability” was then evaluated as the average of all such pairwise separation measures.
- Multiplicity of Peaks: The number of separate intensity peaks located in the object, as indicated by the separation measures discussed above. A threshold value for the intensity drop was defined (0.45) and peaks were grouped together in bunches which were connected by intensities higher than the threshold. If the number of resulting such groups exceeded 3 it was set to 1, so the only possible values it could take were 1, 2 or 3. This was done because of the very low likelihood of mergers of more than three images at high Galactic latitudes. An object with a larger number of peaks would almost certainly be a galaxy, but the actual number would then be meaningless, so it would be right to set it to 1.
- Ratio of Central to Peak Intensity: In many cases the center of a merger lies in between the centers of the individual objects making it, and the intensity at the geometrical center of the merger is much lower than the overall maximal intensity in the object. This ratio betrays these cases and distinguishes them from the single object case, for which this ratio is normally 1.
- Average Quadrant Intensity Difference, based on sampled ellipses: The sampled ellipses were divided to four groups making up four quadrants, the dividing lines being the major and minor axes. The total intensity in each of these quadrants was measured and all six differences between these quadrants were calculated. The six differences are averaged to produce this single parameter.
- Average Quadrant Area Difference, based on whole image: The area of each quadrant was calculated, where in this case quadrants were defined over the entire object (rather than just the sampled ellipses) and the dividing lines were the x and y axes of the image (rather than its major and minor axes). This parameter is the average of all six area-differences between pairs of quadrants.

Table 3. Classification Results of the ANN (averaged over 10 runs) at High Galactic Latitudes, for all Patterns in Set 2 (training on Set 1). Eyeball Classes are recorded on the vertical axis and ANN Classes on the horizontal axis.

Class	Star	Galaxy	Noise	S+St	St+G	G+G	% HR	% FA
Star	1533	3	0	15	0	0	98.8	1.7
Galaxy	2	616	1	16	17	0	94.5	11.9
Noise	0	3	79	4	8	0	84.0	9.2
St+St	21	17	4	552	21	0	89.8	14.4
St+G	3	56	3	56	72	0	37.9	44.6
G+G	0	4	0	2	12	0	0.0	0.0

As above for all Patterns in Set 1 (training on Set 2).

Class	Star	Galaxy	Noise	St+St	St+G	G+G	% HR	% FA
Star	1543	5	0	11	1	0	98.9	3.4
Galaxy	10	608	3	19	10	0	93.5	12.6
Noise	0	9	83	1	4	0	86.3	9.3
St+St	38	21	3	529	22	0	86.3	13.0
St+G	7	53	3	48	73	0	39.7	39.7
G+G	0	1	0	0	11	0	0.0	0.0

5 TRAINING THE ANN

5.1 ANN Classification at High Latitudes

For an overview of ANNs the reader is referred to Hertz, Krogh & Palmer (1991). In the context of astronomical classification ANNs have been used, e.g., by Odewahn *et al.* (1992); Storrie-Lombardi *et al.* (1992); Serra-Ricart *et al.* (1993); Naim *et al.* (1995), to mention but a few. The ANN architecture we use here is 17:5:6 (5 hidden nodes in a single hidden layer and six output nodes), where each output denotes a specific type of object and output values only roughly approximate Bayesian a-posteriori probabilities for class given data. The ANN was run ten times, each time starting with a different randomisation for the weights, training on set 1 and testing on set 2. Then the procedure was reversed for ten more runs, training on set 2 and testing on set 1. Each collection of ten runs was analysed separately. The output node values were averaged over the ten runs, and the classification of each pattern by the ANN was taken as the class for which the average of the ten runs gave the highest “probability”. Table 3 shows the overall performance of the ANN in terms of classification matrices. Here, and in all subsequent classification matrices shown in this paper, eyeball classes appear on the vertical axis, each taking up a row in the matrix, and the resulting ANN classes appear on the horizontal axis, each taking up a column. Successes (“hits”) are recorded on the diagonal and all off-diagonal terms are misclassifications. Also shown in table 3 are the “Hit Rate” and “False Alarm Rate” for each class. The hit rate is defined as the fraction of successful classifications out of all patterns belonging to a given class, e.g., the fraction of objects classified by eye as galaxies which were assigned the same class by the ANN:

$$(3) \quad HR_i = 100 \times \frac{C_{ii}}{\sum_j C_{ij}},$$

where C is the classification matrix. The false alarm rate is the fraction of contaminating patterns, e.g., the fraction of patterns classified by eye as non-stellar, which were misclassified by the ANN as stars, out of all patterns the ANN called stars:

$$(4) \quad FA_j = 100 \times \frac{\sum_{i \neq j} C_{ij}}{\sum_i C_{ij}}.$$

The separation of stars from galaxies is almost perfect, with the very few mistakes being mostly cases in which the eyeballing was uncertain to begin with. As expected, there is some mixing between stars and stellar mergers, and between galaxies and star-galaxy mergers. The galaxy-galaxy merger class is not well defined at all, probably due to the very small number of cases belonging to this class. From the point of view of

Table 4. Classification Results of the ANN for Images larger than $30''$ in Set 2 (training on Set 1). Eyeball Classes are recorded on the vertical axis and ANN Classes on the horizontal axis.

Class	Star	Galaxy	Noise	St+St	St+G	G+G	% HR	% FA
Star	243	0	0	2	0	0	99.2	3.2
Galaxy	2	196	0	3	9	0	93.3	7.1
Noise	0	0	15	1	0	0	93.8	0.0
St+St	6	3	0	76	2	0	87.4	16.5
St+G	0	10	0	9	3	0	13.6	82.4
G+G	0	2	0	0	3	0	0.0	0.0

As above for Images smaller than $30''$ in Set 2 (training on Set 1).

Class	Star	Galaxy	Noise	St+St	S+G	G+G	% HR	% FA
Star	1290	3	0	13	0	0	98.8	1.4
Galaxy	0	420	1	13	8	0	95.0	13.9
Noise	0	3	64	3	8	0	82.1	11.1
St+St	15	14	4	476	19	0	90.2	14.1
St+G	3	46	3	47	69	0	41.1	38.9
G+G	0	2	0	2	9	0	0.0	0.0

creating a galaxy catalogue, the most worrying numbers are the misclassified galaxies (incompleteness) and the contamination of galaxies by non-galaxian images. Although both of these numbers are small here, one must bear in mind that at lower Galactic latitudes the incidences of mergers is much higher and with them the contamination rate is expected to rise. Of the 615 stellar mergers in set 2, 17 were mistaken to be galaxies (2.8%), and so were 21 of the 613 (3.4%) of the stellar mergers in set 1.

In order to check the dependence of the ANN performance on the sizes of the images each set was split in two, one part containing images whose major axis was larger than $30''$ and the other containing images smaller than $30''$. The results for both data sets are shown in tables 4 and 5. The hit rate for galaxies improves in one set and decreases slightly in the other for the larger images, and their contamination by non-galaxian images drops from 3.3% to 1.4% in set 2, and rises from 5.3% to 6.6% in set 1, so there is no overall improvement. Following Odewahn *et al.* (1992), the next thing to try is separating the images into two size groups before training, and train a separate ANN for each size group. The dataset was split in two, including all images larger than $25''$ in one group, and all images smaller than $30''$ in the other, so there is some overlap between the groups. As expected, there were many more objects in the “small” sets than in the “big” sets. However, the results (tables 6 and 7) show that there is virtually no change in the performance of the ANN, and so the conclusion is that the chosen parameters describe the various classes of objects well regardless of image size, down to the limit chosen to begin with.

It is interesting to compare the performance of the ANN at high Galactic latitudes with the result of Maddox *et al.* (1990a), who used empirical functional dependencies between various APM-measured parameters. Their sample was defined differently, by imposing an area limit of 16 pixels, regardless of the shape of the image. They used scans with a finer resolution, of roughly 0.5 arcsec/pixel, and the chosen size limit implies the inclusion of fainter objects. The parameters they used were automatically measured by the APM machine and do not allow the analysis of merged objects. For the separation between stars and non-stars they got a hit rate of 90-95% (depending on magnitude) and a contamination level of 5-10%. Comparing this with the ANN hit rate of over 99%, it appears that the ANN is doing much better. However, it is hardly surprising, because of the inclusion of fainter and smaller objects in their sample.

5.2 Extension to Lower Latitudes

Automated classifications of the images at low Galactic latitudes were first done using the ANNs trained on the high-latitude images, in order to see whether the parameters measured at high latitudes describe the distinct classes as well in low latitudes. The results are shown in table 8.

It is evident that the success rates are lower for all classes. While the hit rates for stars and galaxies are still

Table 5. As above for Images larger than 30'' in Set 1 (training on Set 2).

Class	Star	Galaxy	Noise	St+St	St+G	G+G	% HR	% FA
Star	254	2	0	3	0	0	98.1	5.9
Galaxy	0	183	2	0	5	0	96.3	13.7
Noise	0	4	18	0	0	0	81.8	18.2
St+St	15	8	0	70	4	0	72.2	12.5
St+G	1	15	2	7	11	0	30.6	50.0
G+G	0	0	0	0	2	0	0.0	0.0

As above for Images smaller than 30'' in Set 1 (Training on Set 2).

Class	Star	Galaxy	Noise	St+St	St+G	G+G	% HR	% FA
Star	1299	3	0	8	1	0	99.1	2.9
Galaxy	10	425	1	19	5	0	92.4	12.2
Noise	0	5	70	1	4	0	87.5	6.7
St+St	23	13	3	459	18	0	89.0	13.1
St+G	6	38	1	41	62	0	41.9	37.4
G+G	0	0	0	0	9	0	0.0	0.0

Table 6. Classification Results of the ANN for Big Images Datasets; Trained on Set 1 and Tested on Set 2.

Class	Star	Galaxy	Noise	St+St	St+G	G+G	% HR	% FA
Star	303	1	0	2	0	0	99.0	6.2
Galaxy	0	231	3	3	5	0	95.5	8.0
Noise	0	3	16	0	0	0	84.2	20.0
St+St	17	2	0	96	3	0	81.4	18.6
St+G	3	11	1	14	9	0	23.7	47.1
G+G	0	3	0	3	0	0	0.0	0.0

As above, Trained on Set 2 and Tested on Set 1.

Class	Star	Galaxy	Noise	St+St	St+G	G+G	% HR	% FA
Star	303	1	0	13	0	0	95.6	2.6
Galaxy	1	220	1	1	2	0	97.8	9.5
Noise	0	2	26	0	0	0	92.9	10.3
St+St	7	2	0	108	1	0	91.5	18.2
St+G	0	17	2	9	7	0	20.0	50.0
G+G	0	1	0	1	4	0	0.0	0.0

rather good, the contamination of both by stellar mergers is huge. One factor which could contribute to this high contamination rate is obvious from figure 3, namely the fact that class priors are markedly different between the high Galactic latitude patches and those at low Galactic latitudes. Since the ANN roughly approximates Bayesian a-posteriori probabilities when it finishes training, it should in principle be easy to correct for this factor by dividing all probabilities by the class priors at high latitudes and multiplying them instead by the priors corresponding to the low latitudes. This was done next, and the results are shown in table 9. As can be seen, this indeed improves the results, but they are still not nearly as good as those for the high latitudes. Another possible contributor to the lower success rates is the difference in appearance of objects at high and

Table 7. Classification Results of the ANN for Small Images Dataset; Trained on Set 1 and Tested on Set 2.

Class	Star	Galaxy	Noise	St+St	St+G	G+G	% HR	% FA
Star	1332	3	0	13	2	0	98.7	2.1
Galaxy	7	466	3	14	9	0	93.4	14.0
Noise	0	5	83	2	6	0	86.5	15.3
St+St	19	20	7	509	21	0	88.4	12.8
St+G	3	47	5	45	72	0	41.9	39.5
G+G	0	1	0	1	9	0	0.0	0.0

As above, Trained on Set 2 and Tested on Set 1.

Class	Star	Galaxy	Noise	St+St	St+G	G+G	% HR	% FA
Star	1410	2	0	14	0	0	98.9	1.7
Galaxy	4	464	0	13	7	0	95.1	11.6
Noise	0	6	68	1	5	0	85.0	8.1
St+St	15	9	1	487	24	0	90.9	14.4
St+G	6	42	4	54	55	0	34.2	45.0
G+G	0	2	1	0	9	0	0.0	0.0

Table 8. Classification Results for All Objects of Low Galactic Latitudes. The ANN was Trained on Set 2 of the High Galactic Latitude Data.

Class	Star	Galaxy	Noise	St+St	St+G	G+G	% HR	% FA
Star	97	2	0	12	1	0	86.6	71.0
Galaxy	1	18	0	1	2	0	81.8	78.3
Noise	0	0	9	1	1	0	81.8	10.0
St+St	229	49	0	450	39	0	58.7	16.4
St+G	7	13	1	74	20	0	17.4	68.8
G+G	0	1	0	0	1	0	0.0	0.0

As above, with the ANN Trained on Set 1 of the High Galactic Latitude Data.

Class	Star	Galaxy	Noise	St+St	St+G	G+G	% HR	% FA
Star	97	3	1	10	1	0	86.6	67.6
Galaxy	0	21	0	0	1	0	95.5	85.2
Noise	0	2	4	1	4	0	36.4	81.0
St+St	199	87	15	434	32	0	56.6	16.2
St+G	3	28	1	73	10	0	8.7	79.6
G+G	0	1	0	0	1	0	0.0	0.0

Table 9. Classification Results for All Objects of Low Galactic Latitudes. The ANN was Trained on Set 1 of the High Galactic Latitude Data and the Priors were Corrected to Represent the Low Latitude Distribution of Classes.

Class	Star	Galaxy	Noise	St+St	St+G	G+G	% HR	% FA
Star	96	0	0	15	1	0	85.7	68.0
Galaxy	1	10	0	7	4	0	45.5	61.5
Noise	0	0	5	4	2	0	45.5	0.0
St+St	199	12	0	525	31	0	68.4	17.6
St+G	4	3	0	86	22	0	19.1	63.9
G+G	0	1	0	0	1	0	0.0	0.0

As above, the ANN Trained on Set 2 of the High Galactic Latitude Data.

Class	Star	Galaxy	Noise	St+St	St+G	G+G	% HR	% FA
Star	95	2	1	14	0	0	84.8	64.9
Galaxy	1	14	0	4	3	0	63.6	70.8
Noise	0	0	5	4	2	0	45.5	37.5
St+St	173	24	2	543	25	0	70.8	16.3
St+G	2	7	0	84	22	0	19.1	58.5
G+G	0	1	0	0	1	0	0.0	0.0

low latitudes. The fact that correcting the priors did not solve the problem completely means that this factor was important as well. The conclusion was that a separate ANN should be trained on the low latitude data.

A second ANN was then trained on half the low latitude data and tested on the other half (10 times over, as before), and then the order was reversed. Results are shown in table 10. The hit rates for stars and galaxies are still not very high this time, but the false alarm rates have gone very low, especially for galaxies. The main errors with identifying stars is in separating them from stellar mergers, not from other classes. While galaxies are clearly incomplete, they are only little contaminated by stellar mergers. Of course, the number of galaxies is small, and so even one contaminating stellar merger would raise the contamination level significantly. Nevertheless, there are many stellar mergers and none of them contaminates the galaxy class.

5.3 Using The “Probabilities”

Up to this point the only use of the actual “probabilities” was to determine which is the most likely class for any given object. Given a sample of objects with no eyeball classes one could indeed look no further than the most probable class for each of them. However, examining only the winning class will result in incompleteness, which could be a serious problem. It is interesting to see whether the incompleteness could be reduced by examining the probability of belonging to other classes as well. In table 11 each entry represents, as before, a combination of a given eyeball class (row) and an ANN class (column). The actual value of each entry is the probability of the ANN assigning the eyeball class, averaged over all cases corresponding to that given combination of

Table 10. Classification Results at Low Galactic Latitudes. The ANN was Trained and tested on Low Galactic Latitude Data, Training on Set 3 and Testing on Set 4.

Class	Star	Galaxy	Noise	St+St	St+G	G+G	% HR	% FA
Star	28	0	0	32	0	0	46.7	28.2
Galaxy	0	4	0	4	4	0	33.3	0.0
Noise	0	0	3	2	0	0	60.0	0.0
St+St	11	0	0	371	2	0	96.6	19.0
St+G	0	0	0	49	5	0	9.3	54.5
G+G	0	0	0	0	0	0	0.0	0.0

As above, the ANN Trained on Set 2 of the Low Galactic Latitude Data.

Class	Star	Galaxy	Noise	St+St	St+G	G+G	% HR	% FA
Star	19	0	0	33	0	0	36.5	40.6
Galaxy	0	4	0	4	2	0	40.0	0.0
Noise	0	0	3	2	1	0	50.0	25.0
St+St	13	0	1	366	3	0	95.6	21.5
St+G	0	0	0	59	2	0	3.3	75.0
G+G	0	0	0	2	0	0	0.0	0.0

Table 11. Averaged Output Values at Low Galactic Latitudes. The ANN was Trained on Set 1 of the Low Galactic Latitude Data and Tested on Set 2 of the Low Latitude Data.

Class	Star	Galaxy	Noise	St+St	St+G	G+G
Star	0.56	0	0	0.20	0	0
Galaxy	0	0.43	0	0.14	0.25	0
Noise	0	0	0.41	0.31	0	0
St+St	0.38	0	0	0.75	0.28	0
St+G	0	0	0	0.17	0.46	0
G+G	0	0	0	0	0	0

As above, the ANN Trained on Set 2 of the Low Galactic Latitude Data.

Class	Star	Galaxy	Noise	St+St	St+G	G+G
Star	0.62	0	0	0.22	0	0
Galaxy	0	0.51	0	0.08	0.18	0
Noise	0	0	0.39	0.15	0.25	0
St+St	0.35	0	0.29	0.76	0.33	0
St+G	0	0	0	0.18	0.42	0
G+G	0	0	0	0	0	0

eyeball/ANN classes. To make this clearer, examine the second row in the upper table, corresponding to eyeball class “galaxy”: The entry corresponding to ANN class “galaxy” has the value 0.43, which is the average value of the “galaxy” output node when the ANN succeeds in classifying eyeball galaxies correctly. For comparison, eyeball galaxies that are misclassified by the ANN as either stellar mergers or star-galaxy mergers average 0.14 and 0.25, respectively, for the “galaxy” output node. The fact that the former of these numbers is smaller than the latter implies that it might be worth considering as galaxy candidates all the objects for which the “galaxy” output node is larger than 0.20 or so, even if the resulting ANN class is not “galaxy”. The reason is that even for misclassifications values larger than 0.20 are more likely to happen for mergers involving a galaxy than for “pure” stellar mergers. Of course, this will mean a rise in the level of contamination for galaxies, but the success rate will benefit.

This analysis allows for more candidates of a given type, potentially reducing the incompleteness, at the possible expense of raising the level of contamination. Where one draws the line depends on where one would like to put the interplay between completeness and contamination. As can be seen in the lower part of table 11, which refers to the second set of runs, the picture is essentially the same but the actual numbers are slightly different. This means that caution ought to be exercised when classifying fresh data on the basis of a given ANN run: One should always make the decision on where to draw the probabilistic lines on the basis of the average probability table corresponding to that particular run.

5.4 Analysis of ANN Weights: Specialisation

It has been claimed in the past that ANNs are objectionable because they are “black boxes” that can not be understood. In fact, mathematically ANNs are much simpler than common tools of the astronomical trade, such as SPH codes for numerical simulations, and their resulting weights can be readily interpreted. As described above, ten different ANNs were trained, starting each with a different set of random weights. In general there may be many more than one set of final weights giving roughly the same minimised error, since the problem has a very large number of degrees of freedom (these ANNs were using a 17:5:6 architecture, with 126 weights each). So, rather than trying to fit the weights from one run to those from another, single runs were examined closely. They were all found to give essentially the same results. Figures 4 and 5 show the weights at the end of one such run. Figure 4 depicts the weights between the input nodes and the hidden nodes, while figure 5 shows the weights connecting the hidden nodes to the outputs. In figure 5 it can be seen that each output performs a unique transformation of the hidden nodes connected to it: The weights connected to each output node “specialise” in picking out the class represented by that node. For example, the most significant contributions to the output node representing stars come from hidden nodes 1 and 2, both with a positive sign. On the other hand, the weights connected to the output node denoting galaxies are most significant for hidden nodes 2 (negative), 4 (negative) and 5 (positive). It also clear that the weights connected to the output node denoting galaxy/galaxy mergers are all very small, which explains why this node is never chosen by the ANN in the post-training classification stage. One can now take this general picture one step back, to try and see which inputs contribute most to each of the hidden nodes. This could tell which input parameters are more important than others, for each class. In figure 4 it can be seen, for example, that hidden node 1 is most influenced by inputs 4 and 5, corresponding to ellipticity and semi-major axis length. Hidden node 2 is most influenced by inputs 6 and 15, which correspond to the spike-trace and to the ratio of central-to-peak intensity. The largest contributions to hidden node 4 are from inputs 1, 2, 7, 9 and 12, corresponding to $\log(\text{area})$, peak intensity, first moment, and light gradients 1-3 and 2-4. Hidden node 5 is mostly dominated by inputs 2, 4, 5 and 6, which are peak intensity, ellipticity, semi-major axis length and the spike-trace.

By nature, the ANN mixes parameters together to find optimal non-linear combinations. It is therefore not to be expected that a “clean” picture of which parameters determine which class should emerge. However, this analysis can help in locating parameters which contribute almost nothing to the classifications, and tell us which parameters are the most important. The picture obviously becomes more complicated when one analyses the connections between the inputs and the hidden layer, but it can be safely stated that classes become decoupled at the hidden layer, where one can see exactly how they separate from each other and which ones (e.g., the galaxy-galaxy mergers in this case) are not well defined.

6 DISCUSSION

Automated star/galaxy separation is not a new application in astronomy, but surprisingly work to date has left much to be desired. Separating stars from everything else is not enough for researchers whose main interest is galaxies, and we show that galaxies can be reliably separated from other non-stellar images at high Galactic latitudes. However, the potential for exciting discoveries is naturally larger in areas that were traditionally avoided, such as fields at low Galactic latitudes. We show that it is possible to perform the separation of galaxies from other objects in the Zone of Avoidance, although the success rates are lower and the contamination higher.

The tool used here in the role of automated classifier is an ANN. Other classifiers exist, of course, and should give similar results with our data and its parametrisation. The choice of a classifier is largely a matter of convenience. Most of the hard work goes into the parametrisation of the problem. Nevertheless, ANNs have probabilistic capabilities that are useful, e.g., in trying to improve detection limits, and they are easy to use and very versatile. It has been claimed in the past that ANNs are slow, complicated and are difficult to understand or interpret. The ANN code used here, which was kindly supplied by B. Ripley, takes few CPU minutes to converge on a conventional workstation and is very easy to implement. The analysis of the ANN weights (§ 5.4

above) shows that ANNs can be understood and provide insight as to which parameters are more important than others.

The methods described here are readily applicable to any number of fields extracted from the DSS. It is quite possible to proceed and catalogue the entire sky in this manner. However, it might be of limited interest to proceed with the high Galactic latitude patches, as the available digitised plates do not go very deep and the sky has been mapped at these latitudes and down to the chosen limiting size. However, it is very interesting and apparently feasible to produce such a catalogue for the Zone of Avoidance, from which target lists for pointed observations of galaxies could be easily prepared. This project will be pursued further once the higher resolution DSS mk II becomes available.

ACKNOWLEDGEMENTS

The work described in this paper constituted one part of my Ph.D. thesis, under the inspirational supervision of Ofer Lahav. I am indebted to him for much insight into ANNs and their statistical nature. I am enormously grateful to Steve Maddox and Steve Odewahn for sharing their experience with me and bearing with me through long discussions. I would like to thank Brian Ripley for allowing me to use his ANN code, and to acknowledge an Isaac Newton studentship which supported me through part of this research.

Figure Captions :

Figure 1 : A 15'x15' Section of one of the Patches taken from Field 646. Compare with figure 2.

Figure 2 : A 15'x15' Section of one of the Low Galactic Latitude Patches. Compare with figure 1.

Figure 3 : Distributions of Eyeball-Classes in the High Latitude and Low Latitude Datasets. Note the total dominance of stellar mergers at low Galactic latitudes.

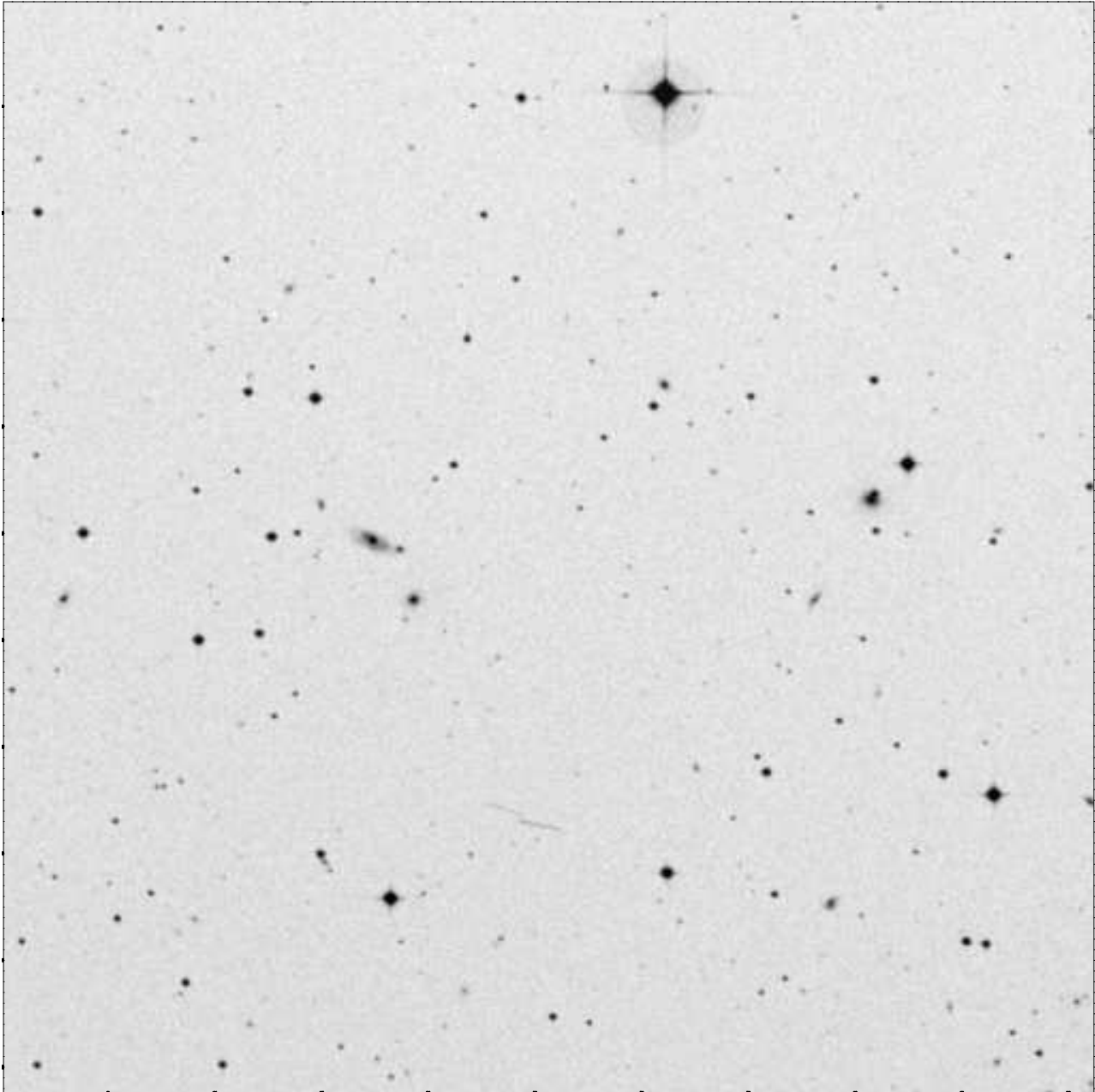
Figure 4 : Weights Connecting Inputs to Hidden Layer Nodes for a Single Run.

Figure 5 : Weights Connecting Hidden Layer Nodes to Outputs for a Single Run.

REFERENCES

- Gunn, J.E., 1995, in: Maddox, S.J. & Aragon-Salamanca, A. (eds.), *Wide Field Spectroscopy and the Distant Universe*, Proceedings of the 35th Herstmonceux conference, Singapore: World Scientific.
- Hertz, J., Krogh, A., & Palmer, R.G., 1991, *Introduction to the Theory of Neural Computation*, Addison-Wesley, California.
- Jarvis, J.F. & Tyson, J.A., 1981, A.J., **86**, 476.
- Kraan-Korteweg, R.C., Loan, A.J., Burton, W.B., Lahav, O., Ferguson, H.C., Henning, P.A. & Lynden-Bell, D., 1994, *Nature*, **372**, 77.
- Lasker, B.M., Struch, C.R., McLean, B.J., Russell, J.L., Jenker, H. & Shara, M.M., A.J., **99**, 2019.
- Maddox, S.J., Sutherland, W.J., Efstathiou, G. & Loveday, J., 1990a, *Mon. Not. R. Astron. Soc.*, **243**, 692.
- Maddox, S.J., Sutherland, W.J., Efstathiou, G. & Loveday, J., 1990b, *Mon. Not. R. Astron. Soc.*, **246**, 433.
- Naim, A., Lahav, O., Sodr e Jr., L. & Storrie-Lombardi, M.C., 1995, *M.N.R.A.S.*, **275**, 567.
- Odehahn, S.C., Stockwell, E.B., Pennington, R.L., Humphreys, R.M. & Zumach, W. A., 1992, A.J., **103**, 318.
- Sebok, W.L., 1979, A.J., **84**, 1526.
- Serra-Ricart, M., Calbert, X., Garrido, L. & Gaitan, V., 1993, A.J., **106**, 1685.
- Slezak, E., Bijaoui, A. & Mars, G., 1988, A. & A., **201**, 9.
- Storrie-Lombardi, M.C., Lahav, O., Sodr e Jr., L. & Storrie-Lombardi, L.J., 1992, *M.N.R.A.S.*, **259**, 8p.

High b



Low b

